Ferroelectricity of Inclusion Compounds of Thiourea with Pyridinium Iodide and Nitrate

ARTICLE *in* THE JOURNAL OF PHYSICAL CHEMISTRY C · APRIL 2009

Impact Factor: 4.77 · DOI: 10.1021/jp9004295

Ferroelectricity of Inclusion Compounds of Thiourea with Pyridinium Iodide and Nitrate

A. Pajzderska,*,† E. Collet,‡ P. Czarnecki,† and J. Wąsicki†

Faculty of Physics, A. Mickiewicz University, ul. Umultowska 85, 61-614 Poznań, Poland, and Université de Rennes 1, Institut de Physique de Rennes, UMR UR1-CNRS 6251, F-35000 Rennes, France

Received: January 15, 2009; Revised Manuscript Received: February 19, 2009

The character of phase transitions in the inclusion compounds of thiourea with pyridinium iodide and nitrate has been analyzed, and a model of ferroelectricity of these compounds has been proposed. Analysis of the temperature dependence of specific heat and intensity of the Bragg peaks has shown that the ferro-paraelectric phase transitions are continuous, in contrast to the nonferroelectric phase transitions. The ferroelectricity of the inclusion systems studied is of the mixed type and has a displacement component and an order−disorder component.

Introduction

Ferroelectrics have always been interesting because of their unique physicochemical properties and have recently become the object of intense studies because of their prospective use in nanodevices.[1−3] A very interesting application of ferroelectrics is the so-called ferroelectric random access memory (FRAM). Much effort is directed toward the search for new ferroelectric materials and their characterization, to extend the range of their use. Ferroelectric crystals in general can be divided into displacement and order−disorder types. In the crystals of displacement type, spontaneous polarization appears as a result of relative displacement of ions or molecules, while in the crystals of order−disorder type, it appears as a result of ordering of electric dipoles of ions or molecules.[4,5] Spontaneous polarization can be determined experimentally from the pyroelectric effect or hysteresis loop. As yet, there have been only a few attempts at calculation of the spontaneous polarization,[6−13] as its calculation is difficult but seems to be informative about the nature of this phenomenon.

Ferroelectric properties have been detected in many inorganic and organic molecular crystals.[4−7,14] In the beginning of the 1990s, ferroelectric properties were found in some pyridinium salts, belonging to a family of ion-molecular crystals with an interionic hydrogen bond. Ferroelectric properties were detected only in the salts whose anions have tetrahedral symmetry: BF_4, ClO_4, ReO_4, and IO_4.[15−20] A characteristic feature of this group of ferroelectrics is a sequence of two-phase transitions, of which the one at the higher temperature is the Curie point.

To explain the nature of ferroelectricity in these salts, spontaneous polarization was calculated for the crystals (PyH)BF_4, (PyH)ClO_4, and (PyH)IO_4.[10−13,21] NMR (^{1}H and ^{2}H) results have shown that in all pyridinium salts the cation reorientations take place around the axis perpendicular to its plane, in the intermediate and low-temperature phases, between the potential energy minima of different values.[19,20] So, on the basis of the cation dynamics, a model of 6-fold potential barrier, of different barrier heights, was assumed for (PyH)BF_4 and (PyH)ClO_4, while for (PyH)IO_4, the shape of the potential for the cation reorientations was established on the basis of the populations of the positions in the pyridinium cation by nitrogen atoms determined by neutron diffraction.[21−24] The temperature dependence of the ^{2}H NMR line shape permitted determination of the populations of the particular potential energy minima and hence also the polarization as a function of temperature. A very good agreement between the measured and calculated values of the spontaneous polarization for (PyH)BF_4, (PyH)ClO_4 (in high- and low-temperature phases), and (PyH)IO_4 (all phases) permits classification of these pyridinium salts to the order−disorder type.[24]

The inclusion systems of thiourea and pyridinium salts are less known ferroelectric crystals. The complexes are ion-molecular systems in which besides the van der Waals interactions also the Coulomb interactions and hydrogen bonds occur. These systems are much more complex than simple pyridinium salts, because of a strong coupling between thiourea making the host lattice and pyridinium cations making the guest lattice. Hitherto four such systems have been recognized with the Cl, Br, I, and NO_3 anions (hereafter denoted as T_2(PyH)Cl, T_2(PyH)Br, T_2(PyH)I, and T_2(PyH)NO_3, respectively).[25−33] All of these systems undergo two-phase transitions as temperature is decreased.[25,28,30,32,34] Recently, ferroelectric properties have been found in the low-temperature phase and intermediate phase of T_2(PyH)I[30,32] and in the low-temperature phase in T_2(PyH)NO_3,[28] but no model of ferroelectricity in these compounds has been proposed. The problem is even more interesting because the complexes (PyH)I and (PyH)NO_3 do not show ferroelectric properties.

The aim of the study was determination of the character of phase transitions, analysis of entropy changes and their relation with the ions dynamics, proposition of the model of ferroelectricity, as well as estimation of polarization values in these systems and its comparison with that proposed for pyridinium salts.

Experimental Section

The compounds were synthesized as described in refs 25, 27. The differential scanning calorimetry measurements were performed as desribed in ref 30. X-ray diffraction was performed on single crystals with typical sizes around 200 × 200 × 500 μm^3. The diffraction experiments were carried out on a Xcalibur 3 four-circle diffractometer (Oxford Diffraction) equipped with a 2D sapphire 3 CCD detector with Mo Kα radiation (λ = 0.71069 Å). The single crystals were mounted in an Oxford

* Corresponding author. E-mail: apajzder@amu.edu.pl.
† A. Mickiewicz University.
‡ Université de Rennes 1.

10.1021/jp9004295 CCC: $40.75
Published on Web 03/20/2009

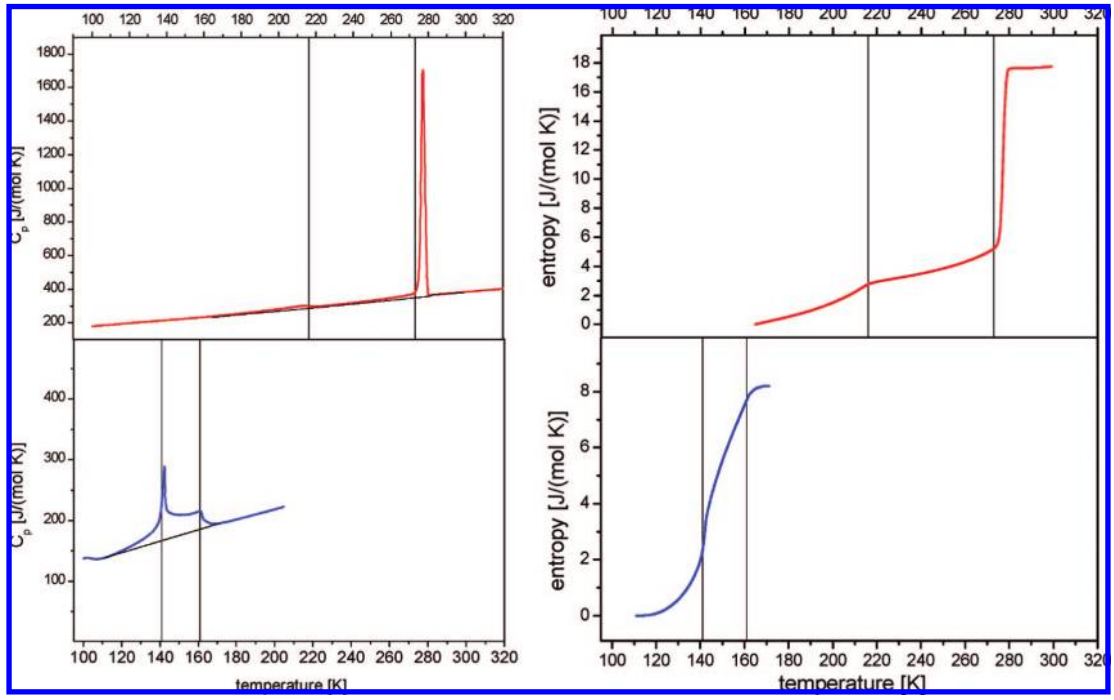

Figure 1. Temperature dependencies of the specific heat and the entropy for $T_2(PyH)NO_3$ (top) and $T_2(PyH)I$[30] (bottom).

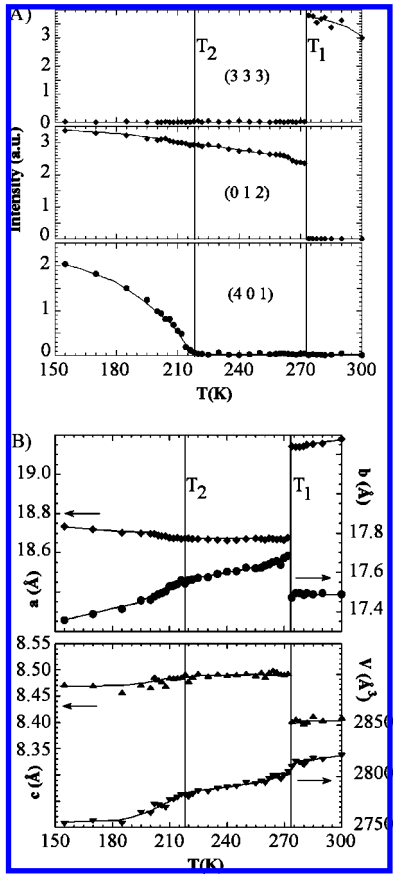

Figure 2. X-ray signatures of the phase transition of $T_2(PyH)NO_3$. (A) Temperature dependence of selected Bragg reflections intensities associated with the change of translation symmetry from HT to INT phase (top) and space group (middle and bottom). (B) Temperature dependence of the lattice parameters *a* for HT and 2*a* for INT and LT and *b* (top), and *c* and volume *V* (bottom) [see also ref 28].

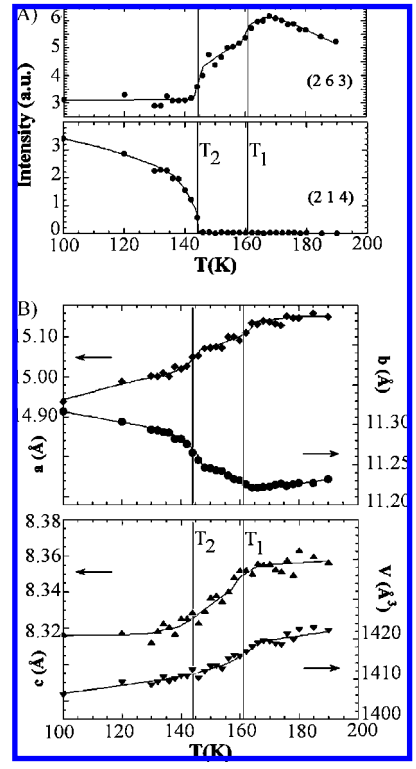

Figure 3. X-ray signatures of the phase transition of $T_2(PyH)I$. (A) Temperature dependence of selected Bragg reflections intensities associated for general reflection (top) and one associated with the symmetry breaking (bottom), and (B) temperature dependence of the lattice parameters *a* and *b* (top), and *c* and volume *V* (bottom) [see also ref 32].

Cryosystems nitrogen-flow cryostat for measurements down to 100 K, with a temperature stability of 0.1 K. The unit cell parameters and the data reduction to obtain Bragg reflections intensities were obtained with CrysAlis software from Oxford Diffraction.

The Structure and the Character of Phase Transitions. DSC measurements were previously performed[27,30] to determine phase transition temperatures. Results of the specific heat

TABLE 1: Crystal Data (Space Groups, Unit Cell Parameters, and *Z* Number) and the Temperature at Which a Given Crystallographic Structure Was Determined for T_2(PyH)I and T_2(PyH)NO_3[a]

	HT	INT	LT
T_2(PyH)I[30]	295 K, *Cmcm*, a = 15.180 Å, b = 11.827 Å, c = 8.375 Å, Z = 4	**155 K, *C*2*cm*, a = 15.022 Å, b = 11.227 Å, c = 8.3410 Å, Z = 4**	**110 K, $P2_1cn$, a = 14.8600 Å, b = 11.2910 Å, c = 8.307 Å, Z = 4**
T_2(PyH)NO_3[28]	293 K, *Pbmn*, a = 19.150 Å, b = 17.402 Å, c = 8.441 Å, Z = 8	250 K, $P2_1/c$, a = 9.319 Å, b = 17.555 Å, c = 8.484 Å, β = 91.14°, Z = 4	**150 K, $P2_1a$ a = 9.354 Å, b = 17.244 Å, c = 8.452 Å, β = 91.22°, Z = 4**

[a] The ferroelectric phases are marked with bold.

measurements by the DSC method for the two inclusion compounds and the entropy obtained from these measurements are given in Figure 1. According to the temperature dependence of entropy (Figure 1), the total change in entropy for T_2(PyH)NO_3 is close to 17.7 J/K·mol, while in T_2(PyH)I it is close to 8.2 J/K·mol. As follows from the specific heat anomalies, both crystals reveal two phase transitions, so they can occur in three phases: high-temperature (HT), intermediate (INT), and low-temperature (LT).

The shape of the specific heat C_p anomaly suggests that in T_2(PyH)NO_3 the phase transition at the higher temperature (T_1 = 273 K) is discontinuous, while that at the lower temperature (T_2 = 216 K) is continuous. In T_2(PyH)I the reverse is true; the phase transition at T_1 = 161 K is continuous, and that at T_2 = 143 K is discontinuous.

To establish more accurately the character of the phase transitions, the temperature dependence of the intensity of selected (*hkl*) Bragg peaks as well as temperature dependence of lattice parameters were performed. For T_2(PyH)NO_3 and T_2(PyH)I, the crystallographic structures together with the temperature dependence of lattice parameters of all of the phases were determined and published in refs 28 and 30.

For T_2(PyH)NO_3, the phase transition at T_1 is associated with a symmetry breaking from the space group *Pbmn* (HT) to $P2_1/c$ (INT) and $P2_1$ (LT) as well as change of translation symmetry from a = 19.15 Å (HT) to a' = 9.319 Å (INT and LT) with $a' = 2a$. Therefore, Bragg reflection (*hkl*) indexed $h = 2n + 1$ in the HT lattice is only present in the HT phase. The discontinuous disappearance of the (333) Bragg reflection at T_1 (Figure 2a) is a direct signature of the discontinuous (first order) nature of this phase transition. The discontinuous appearance of the (012) Bragg reflection is another signature of this phase transition, associated with the loss of the b glide plane between the HT and INT as well as LT phases (Figure 2a). The lattice parameters also show discontinuous variations at T_1 (Figure 2b). The change of space group due to the loss of c glide plane at T_2 is associated with the appearance of (*h*0*l*) Bragg reflections indexed $h + l = 2n + 1$. The continuous variation of the intensity of the (401) peak confirms the continuous (second order) nature of this phase transition, accompanied by continuous changes of lattice parameters (Figure 2a and b).

For T_2(PyH)I, the phase transition at T_1 is associated with a symmetry breaking from the space group *Cmcm* (HT) to *C*2*cm* (INT) and $P2_1cn$ (LT) without change of translation symmetry. Many Bragg reflections such as (263) (Figure 3a) were found to be sensitive to both phase transitions, even though not directly related to symmetry breaking. The change of space group at T_2 due to a change from C to P cell is associated with the appearance of (*hkl*) Bragg reflections indexed $h + k = 2n + 1$. The temperature dependence of the intensity of the (214) peak shows a small jump at T_2. Both phase transitions are accompanied by variations of lattice parameters (Figure 3b), which do not exhibit as large of a jump as for the NO_3 compound. Therefore, T_2(PyH)I shows a weak discontinuous transition at T_2 as compared to a strong discontinuous (first order) one of T_2(PyH)NO_3 at T_1. This statement (conclusion) is also confirmed by C_p measurements (Figure 1).

Table 1 presents the spatial groups, elementary cell parameters, number of molecules and ions in the elementary cell, and the temperatures at which a given crystallographic structure was determined. It should be emphasized that both the thiourea molecules and the pyridinium cations have dipolar moments (Figure 4). The thiourea molecules linked by the N−H···S hydrogen bonds are arranged head-to-tail, forming ribbons along the z axis. The name half-ribbon refers to these thiourea molecules whose C and S atoms are directed in the same way. The mean plane is determined by the heavy atoms (N,C,S) belonging to the half-ribbon (Figure 4). In the LT phase, the angles α (Figure 4) between the mean planes of the two half-ribbons are 37° and 6° for T_2(PyH)NO_3 and 17° for T_2(PyH)I. In the INT phase, these values decrease and become 33° and 0° for T_2(PyH)NO_3 and 12° for T_2(PyH)I. In the HT phase, these angles are different from zero only in T_2(PyH)NO_3 and take the values 45° and 6°.

The planar ribbon made of the thiourea molecules endowed with dipolar moments does not have a resultant dipolar moment; however, the nonplanar (bent) ribbon has a resultant dipolar moment perpendicular to its plane determined by the heavy atoms. In Figure 4, the dipole moments of the thiourea molecules and the resultant moment of the ribbon are marked by arrows.

Four ribbons parallel in pairs make a channel, except for one pair in T_2(PyH)NO_3. The angle made by the mean planes (for all ribbons) and the (001) plane (the cross-section of the channel) is 90° or close to this value. The channel hosts the pyridinium cations. The neighboring stacked cations are not mutually parallel; the angle between the planes of the cations in the column in the LT phase is 7° for T_2(PyH)NO_3 and 15° for T_2(PyH)I, and upon transition from LT to HT these angles increase by 11° for T_2(PyH)I and by 5° for T_2(PyH)NO_3.

For the cations whose nitrogen atom positions in the rings had been determined by the X-ray method, it was possible to determine the mutual orientation of neighbors in the channel. The dipole moments of the neighboring channels in the LT phase make the angle of 142° in T_2(PyH)NO_3 and 78° in T_2(PyH)I. T_2(PyH)I determination of this angle in the INT phase is impossible as the nitrogen atom positions in the cation are not known.

The distances between the heavy atoms in the cation (C, N) and the channel have been determined and implied that the cation (nitrogen atom) in T_2(PyH)NO_3 is the strongest bonded with the anion (the shortest distances). In T_2(PyH)I, the cation is the strongest bonded with the walls made by the thiourea molecules. It should be remembered that in T_2(PyH)I in the LT and INT phases the angles between the thiourea molecules making a ribbon are 17° and 11.6°. Similarly nonplanar channel walls occur in T_2(PyH)NO_3; however, because of the shape of

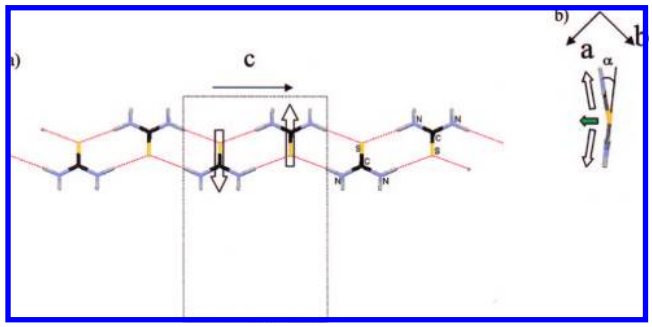

Figure 4. The fragment of the infinite ribbons form from the thiourea molecules linked by N−H···S bonds along the *c* axis (a) and in the *ab* plane (b). H bonds are represented by red dotted lines. The open arrows indicate the dipolar moment of the thiourea molecules (a) and the green one the resultant dipolar moment of the ribbon (b) depending on the angle α between half-ribbons.

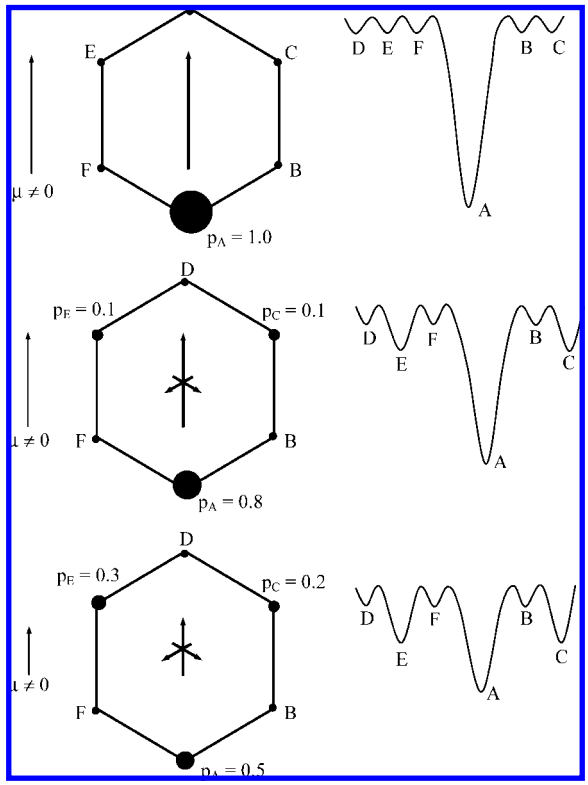

Figure 5. Occupancy of the nitrogen atom of the pyridinium cation in $T_2(PyH)NO_3$ at LT (top), INT (middle), and HT (bottom) phases, the shape of the potential energy function obtained from QNS study, and the resultant dipolar moment of the cation.

the anion (planar and not spherical as in $T_2(PyH)I$), the interactions between the anion and the cation are the strongest.

The phase transitions of the two compounds leading to the polar phases do not involve changes in the crystallographic system, so they are ferroelectric−nonferroelastic. These new ferroelectrics are uniaxial so the spontaneous polarization appears in them in one direction along the 2-fold axis of the $P2_1$ system (*b* axis) in $T_2(PyH)NO_3$ and along the 2-fold axis parallel to *a* of the *C*2*cm* system in $T_2(PyH)I$. The nonferroelectric transition in $T_2(PyH)NO_3$ at T_1 involves a change in the crystallographic system from orthorhombic to monoclinic, so it is a ferroelastic phase transition. The nonferroelectric transition in $T_2(PyH)I$ at T_2 is accompanied by the disappearance of the centering of the elementary cell, so according to the Aizu classification[35] it is a nonferroic phase transition.

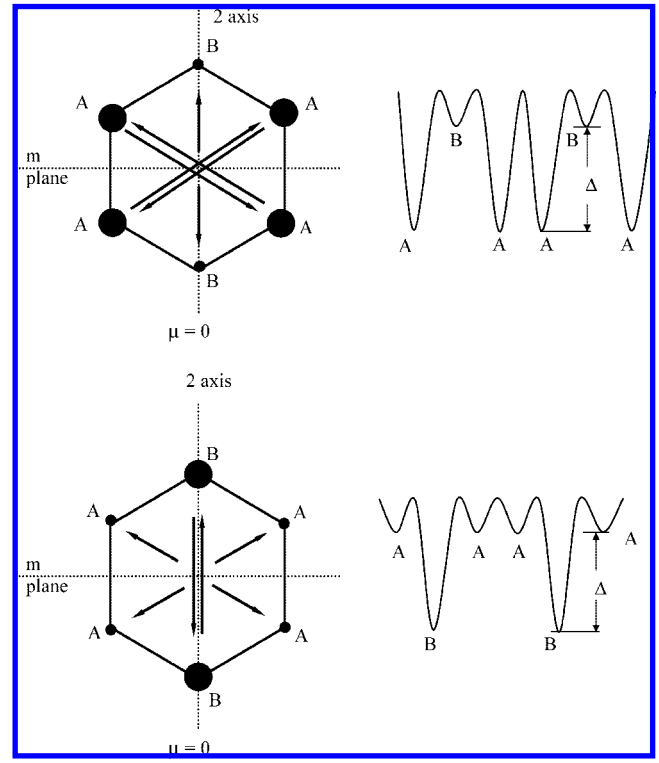

Figure 6. Two possible models (model I, top; model II, bottom) of the shape of the potential energy function and occupancy of the nitrogen atom of the pyridinium cation $T_2(PyH)I$ at HT.

Ion Dynamics and Changes in Entropy. The entropy changes accompanying the phase transitions are important parameters permitting classification of the phase transitions in crystals. A small change in entropy at a phase transition implies its order−disorder character. In the transitions of this type, the entropy change can be found from the formula:

$$\Delta S = R \ln(N_1/N_2) = R \ln(N_1) - R \ln(N_2) \qquad (1)$$

where ΔS is the entropy change, R is the gas constant, N_1 is the number of equilibrium configurations of the disordered phase, and N_2 is the number of equivalent configurations of the ordered or partly disordered phase. If in the disordered phase the reorientation takes place between the inequivalent minima of potential energy, the entropy change is given by:[36]

$$\Delta S = R \sum p_i \ln(1/p_i) - R \sum P_j \ln(1/P_j) \qquad (2)$$

where p_i is the probability of population of the *i*th minimum of the potential energy in the disordered phase, and P_j is the probability of population of the *j*th minimum of the potential energy in the ordered phase. The calculation of entropy values and changes requires the knowledge of the potential shape and probability of population. These data can be obtained from earlier studies. The ^1H NMR results have shown that in the inclusion compounds $T_2(PyH)I$ and $T_2(PyH)NO_3$ the pyridinium cation undergoes reorientation about the axis perpendicular to its plane through inequivalent barriers of potential energy.[26,27] On the basis of these results, the value of the energy difference between the shallow and deep minima of the potential energy, Δ, was calculated. The ^2H NMR measurements have proved an additional reorientation of the cation, the out-of-plane movement, in the HT and INT phases of $T_2(PyH)NO_3$.[29]

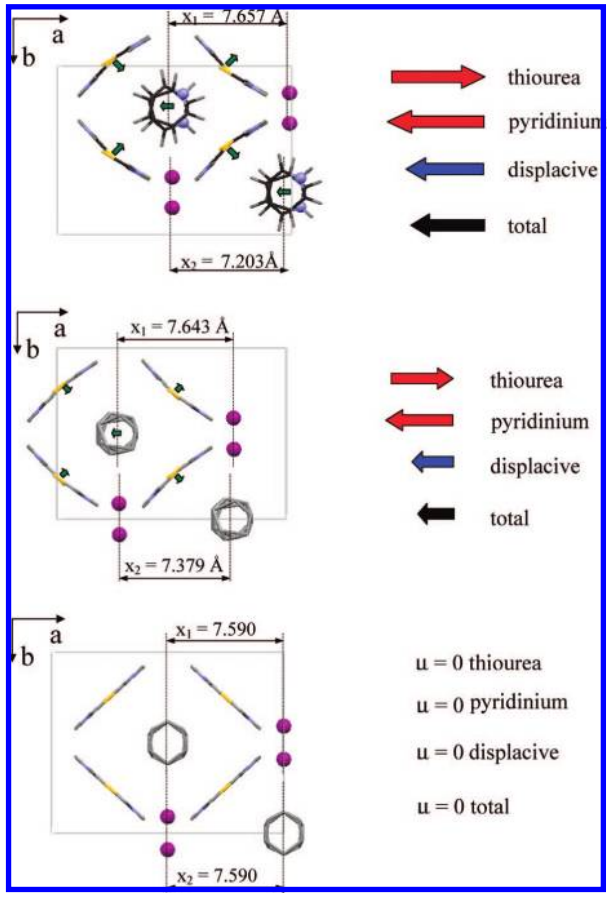

Figure 7. Molecular arrangement in the three phases of $T_2(PyH)I$ (LT phase, top; INT phase, middle; HT phase, bottom) along the *c* axis (in the *ab* plane). The arrows indicate the resultant dipolar moment of individual ribbons of thiourea molecules and that of the cations in the elementary cell. The arrows on the right-hand side of the figure indicate the resultant dipolar moment of all of the ribbons of thiourea molecules and all of the cations, the dipolar moment originating from the mutual shift of the ions, and the total dipolar moment.

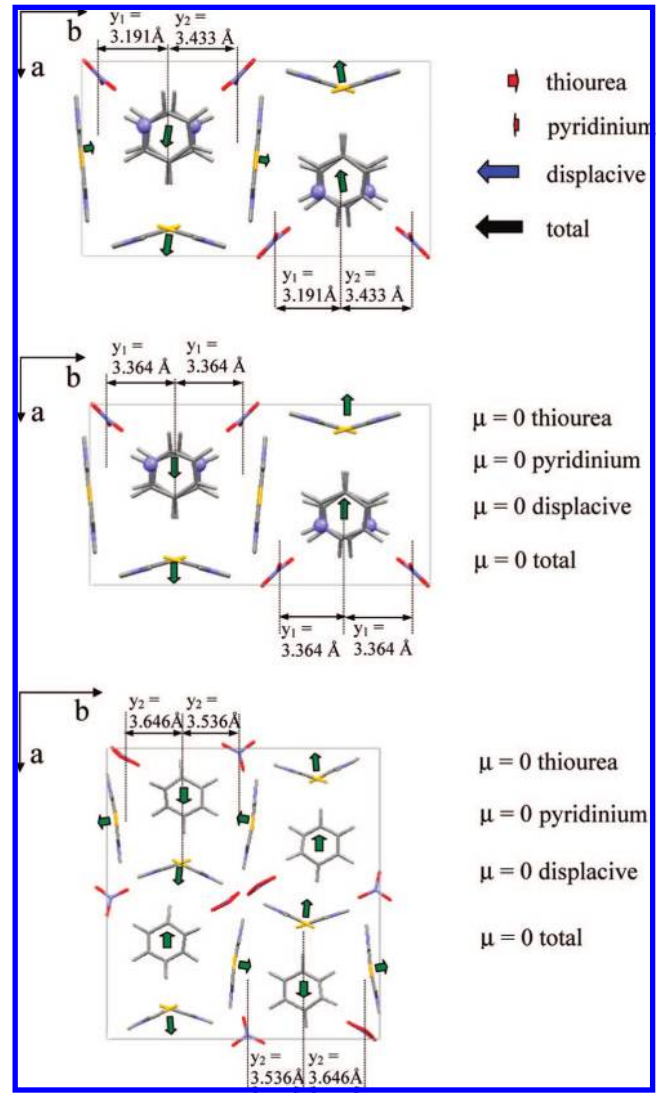

Figure 8. Molecular arrangement in the three phases of $T_2(PyH)NO_3$ (LT phase, top; INT phase, middle; HT phase, bottom) along the *c* axis (in the *ab* plane). The arrows indicate the resultant dipolar moment of individual ribbons of thiourea molecules and that of the cations in the elementary cell. The arrows on the right-hand side of the figure indicate the resultant dipolar moment of all of the ribbons of thiourea molecules and all of the cations, the dipolar moment originating from the mutual shift of the ions, and the total dipolar moment.

The analysis of the QNS data performed for $T_2(PyH)NO_3$ in the HT and INT phases by means of a jump model permitted the determination of the potential energy barriers in these phases.[31] The out-of-plane cation reorientations have been found to take place between two potential energy minima of different values, characterized by the probability of population of 0.8 and 0.2 in the HT phase at 300 K. The in-plane reorientation takes place between unequivalent minima separated by 120°. Figure 5 presents the shape of the potential energy for the cation reorientation in plane and the populations of the potential energy minima by nitrogen atoms. In the INT phase, the population is equal, $p_A = 0.8$, $p_C = p_E = 0.1$, while in HT, $p_A = 0.5$, $p_C = 0.3$, and $p_E = 0.2$.

According to the preliminary analysis of the QNS results obtained for $T_2(PyH)I$, in the HT phase, the cation reorientations about the axis perpendicular to its plane take place between the potential energy minima separated by 180°.[37] On the other hand, the site symmetry of the cation in this phase is 2/*m*, which suggests that the pyridinium cation performs reorientation between two deep and four shallow minima or two shallow and four deep ones (Figure 6). The value of Δ obtained from ^1H NMR measurements is 6 kJ/mol.[26] The QNS measurements have shown that also in the HT and INT phases of T_2PyHI the out-of-plane motion of the cation takes place. The site symmetry of the cation in the HT phase implies that this motion takes place between the equivalent minima of potential energy.

Substitution of the probability of population of the potential energy minima for the in-plane cation reorientation in the HT and INT phases in $T_2(PyH)NO_3$ to eq 2 and assuming that in LT the cation takes only one position, we get the entropy values of 8.6 and 5.3 J/K·mol. A similar procedure for the out-of-plane cation reorientation in the HT phase gives the entropy of 4.2 J/K·mol. As we do not know the probabilities of population of the potential energy minima in the INT phase for the out-of-plane cation reorientation, we are not able to calculate the entropy change related to this motion. It is expected to be much lower than that obtained for the HT phase as the asymmetry of the population of the two minima increases with decreasing temperature, and in the LT phase only one minimum is populated. As follows from the X-ray studies, in the HT phase of $T_2(PyH)NO_3$, every second anion is disordered. The contribution of the disordered anions in the entropy change is $1/2R \ln(2)$

TABLE 2: Dipolar Moments μ and Spontaneous Polarization P of the Elementary Cell

	T_2(PyH)I					T_2(PyH)NO_3			
	LT		INT		HT	LT		INT	HT
	μ [D]	P [μC/cm^2]	μ [D]	P [μC/cm^2]	μ [D]	μ [D]	P [μC/cm^2]	μ [D]	μ [D]
thiourea	5.24	1.26	3.77	0.89	0	0.57	0.14	0	0
pyridinium cation	−5.46	−1.31	−4.09	−0.97	0	−0.25	−0.06	0	0
displacive	4.36	1.04	2.55	0.60	0	2.32	0.57	0	0
total	4.15	0.99	2.21	0.52	0	2.64	0.65	0	0

= 2.9 J/K·mol, so the total entropy change in the HT phase is 8.6 + 4.2 + 2.9 = 15.7 J/K·mol and only a little lower than the experimental value of 17.7 J/K·mol. The volume entropy related to the discontinuous phase transition to the HT phase was not taken into account.[38] The entropy change in the INT phase (neglecting the out-of-plane motion of the cation) is 5.3 J/K·mol and is in good agreement with the experimental value of 4.9 J/K·mol.

Figure 6 presents the two probable models of the potential energy barriers for the in-plane cation reorientation in the HT phase of T_2PyHI. With the experimentally found Δ value, the probabilities of the potential minima populations can be found from the formulas:

$$p_A = 1/(g_A + g_B \exp(-\Delta/RT)) \quad (3a)$$

$$p_B = \exp(-\Delta/RT)/(g_A + g_B \exp(-\Delta/RT)) \quad (3b)$$

where g_A and g_B stand for degeneration of the potential energy minima of the population probabilities of p_A and p_B.

Substituting Δ = 6 kJ/mol into eqs 3a and 3b, the values of p_1 and p_2 are found: for the model I, $p_A = 0.248$, $p_B = 0.003$, while for the model II, $p_A = 0.488$ and $p_B = 0.006$. From eq 2, the change in entropy for both models of the potential energy is obtained. For model 1, the entropy change is 12 J/K·mol, while for model 2 it is 6.8 J/K·mol. As the entropy change in model considerably exceeds the experimental value, we assume that model 2 gives a correct description of the in-plane cation reorientation. It should be noted that the QNS studies correspond much better to this model of the cation reorientation. Taking into account the entropy change related to the out-of-plane cation motion (between two equivalent potential energy minima) estimated as R ln(2) = 5.7 J/K·mol, the total entropy change in the HT phase is 5.9 + 5.7 = 11.6 J/K·mol. This value is greater than the experimental 8.2 J/K·mol. The difference can be explained by the fact that in determination of the entropy change, the integration of the temperature dependence of the specific heat $C_p(T)$ could be performed only in the temperature range over which the DSC apparatus permitted measurements of C_p, and this limitation led to a certain decrease in the entropy value.

The above-analyzed shapes of the potential of the cation reorientation permitted determination of the entropy change, and hence the character of the phase transitions, and were helpful in the explanation of the nature of ferroelectricity in the compounds studied.

The Model of Ferroelectricity. Figures 7 and 8 present the projection of the elementary cell onto the *xy* plane, for all phases of T_2(PyH)I and T_2(PyH)NO_3. The arrows indicate the resultant dipolar moments of the ribbons and the pyridinium cations belonging to the same column.

The resultant dipolar moment along the *z* axis (along the channel) was zero for all of the phases of the two compounds because of the symmetry. In the LT phase of T_2(PyH)I, the resultant dipolar moment (whose contributions come from four nonplanar ribbons in the elementary cell) is directed along the axis *a*, while the resultant dipole moment from the four cations is directed along the axis $-a$. The direction of the dipole moment originating from the relative shift of the cation and the anion is also the same. Figure 7 gives the distances between the centers of the nearest anions and cations along the axis *a* (denoted as x_1 and x_2). They differ by $\Delta x = x_1 - x_2 = 0.454$ Å. In the INT phase, the situation is qualitatively similar. The dipole moment from the nonplanar ribbons is smaller than in the LT phase because of a decrease in the angle of their bent. The distances between the centers of the nearest cations and anions have changed, and the difference $\Delta x = x_1 - x_2 = 0.264$ Å. According to the XRD results, the cation in this phase is disordered. As follows from NMR measurements, the cation undergoes reorientation about the axis perpendicular to its plane through inequivalent potential energy barriers (Figure 6). Such a reorientation causes a reduction of the dipole moment of individual cations and hence also the resultant dipole moment of the elementary cell (originating from the cations); however, the direction of the resultant dipole moment is the same as in the LT phase.

In the HT phase the ribbons are planar, so they bring zero contribution to the resultant dipolar moment of the elementary cell. The dipolar moment of the cations is averaged to zero because of their reorientation about the axis perpendicular to their plane, through inequivalent potential energy barriers of the shape presented in Figure 6. As the distances between the centers of the nearest cations and anions are the same in the elementary cell, thus $\Delta x = 0$, and there is no dipole moment originating from the shift of charges (Figure 8).

To estimate the contributions of individual components of the dipolar moment in particular phases, we assumed that the dipole moment of the thiourea molecule is 6.5 D and the dipole moment of the pyridinium cation as 2 D. The dipole moment values were calculated via the Gaussian package, assuming the geometry of the systems following from the XRD studies, and the values are consistent with those reported by other authors.[39,40] The results are given in Table 2.

In the LT phase of T_2(PyH)I, the contributions of the dipole moments originating from the cations and ribbons almost cancel each other, and the resultant dipolar moment of the elementary cell originates mainly from the mutual shift of the cations and anions. In the INT phase, the dipole moments originating from the cations and ribbons decrease because of the cations motion and a decrease in the angle of the ribbons bending. Exact calculation of the decrease in the dipole moment because of the cations motion is very difficult, so we have estimated that the dipole moment in the INT phase has decreased by 25% of its value from the LT phase. Under this assumption, in the INT phase, the resultant dipolar moment of the elementary cell decreases by one-half, comes mainly from the mutual shift of the ions, and is directed along the axis *a*. In the HT phase of

T_2(PyH)I, the resultant dipolar moment of the elementary cell is zero, and all of its components are also zero.

As follows from Figure 8, in the LT phase of T_2(PyH)NO_3, the resultant dipolar moment originating from the nonplanar ribbons is directed along the axis b, while the resultant dipolar moment from the cations is directed along $-b$. A detailed analysis of the cations and anions positions in the elementary cell has shown that they are mutually shifted. In Figure 8, the closest distances between the cations and anions along the axis b are denoted as y_1 and y_2.

Thus, $\Delta y = y_1 - y_2 = 0.242$ Å. As both cation−anion pairs in the elementary cell are shifted in the same direction, to estimate the dipolar moment originating from the shift the value of $2\Delta y$ is used. In the INT phase, the resultant dipolar moment originating from the ribbons is zero. The two walls are planar, and the dipolar moments of the two nonplanar ribbons cancel out. Similarly, the dipolar moments originating from the cations cancel out. The nearest cation−anion distances in the elementary cell are the same, so the component of the dipolar moment related to the shift of ions is also zero. In the HT phase, all of the walls of the elementary cell are nonplanar, but their dipolar moments cancel each other similarly as the dipolar moments of the cations. The nearest cation−anion distances are different in the elementary cell, and Δy is 0.071 Å; however, as in this phase the shifts are symmetrical, in contrast to those in the LT phase, the relevant dipolar moments are of the same value but in opposite directions so they cancel out. As follows from analysis of the data presented in Table 2, the dipolar moment originating from the thiourea molecules in the LT phase of T_2(PyH)NO_3 is nearly twice greater than that originating from the pyridinium cations. The dipolar moment originating from the mutual shift of the ions is approximately by one-half lower than that in the LT phase of T_2(PyH)I, so the resultant dipolar moment of the elementary cell in this phase is greater for T_2(PyH)I. The resultant dipolar moments were expressed in the value of spontaneous polarization, and the results are given in Table 2. The spontaneous polarizations of the two compounds have been estimated as about 1 μC/cm^2. The spontaneous polarization measured in pyridinium salts varied from about 1 to 3 μC/cm^2,[13,23,41,42] whereas in a very well-known ferroelectric, triglycine sulfate, TGS, crystal, the spontaneous polarization reaches about 3 μC/cm^2.[43]

The above analysis of the dipolar moments has shown that the spontaneous polarization of the compounds studied originates from both mutual shift of the ions and the orientational ordering of the cations and ribbons made of the thiourea molecules.

Conclusions

The above-discussed results and analyses permit us to draw the following conclusions.

(1) Introduction of simple pyridine salts ((PyH)I, (PyH)NO_3), which are not ferroelectric, into the matrix made of the thiourea molecules gives an inclusion compound showing ferroelectric properties.

(2) The two inclusion compounds studied show two phase transitions, similarly as the ferroelectric pyridinium salts ((PyH)IO_4, (PyH)ReO_4, (PyH)ClO_4, (PyH)BF_4). In T_2(PyH)I, the phase transition at the higher temperature is the Curie point, similarly as in the pyridinium salts. In T_2(PyH)NO_3, the Curie point corresponds to the temperature of the low-temperature phase transition.

(3) Analysis of the temperature dependence of specific heat and intensity of the Bragg peaks has shown that the ferro-paraelectric phase transitions are continuous, in contrast to the nonferroelectric phase transitions.

(4) The entropy changes in the systems studied can be explained in terms of the model of reorientation of the pyridinium cations through the inequivalent potential energy barriers.

(5) The ferroelectricity of the inclusion systems studied is of the mixed type and has a displacement component and an order−disorder component in contrast to pure pyridinium salts, which belong to the order−disorder ferroelectrics.

Acknowledgment. This work has been partially financed by the Ministry of Science and Higher Education of Poland from 2006−2008 funds, grant no. N202 134 31/2331.

References and Notes

(1) Uchino, K. *Ferroelectric Devices*; CRC Press: New York, 2000.
(2) Yuhuan, X. *Ferroelectric Materials and Their Applications*; Elsevier Science Pub. Co.: New York, 1991.
(3) Scott, J. F. *Ferroelectrics* **2005**, *316*, 13–21.
(4) Connolly, T. F.; Turner, E. *Ferroelectric Materials and Ferroelectricity*; IFI/Plenum: New York, 1970.
(5) Gonzalo, J. A.; Jiménez, B. *Ferroelectricity: The Fundamentals Collection*; Wiley-VCH: New York, 2005.
(6) Katrusiak, A.; Szafrański, M. *Phys. Rev. Lett.* **1999**, *82*, 576.
(7) Szafrański, M.; Katrusiak, A.; McIntyre, G. J. *Phys. Rev. Lett.* **2002**, *89*, 5507.
(8) Szafrański, M. *Phys. Rev. B* **2005**, *72*, 054122.
(9) Szafrański, M. *Solid State Commun.* **1990**, *75*, 535.
(10) Fojud, Z.; Goc, R.; Jurga, S.; Kozak, A.; Wąsicki, J. *Mol. Phys.* **2003**, *101*, 1469.
(11) Beck, B.; Villanueva-Garibay, J. A.; Muller, K.; Roduner, E. *Chem. Mater.* **2003**, *15*, 173.
(12) Vujosevic, D.; Muller, K.; Roduner, E. *J. Phys. Chem. B* **2006**, *110*, 8598.
(13) Wąsicki, J.; Fojud, Z.; Czarnecki, P.; Jurga, S. *Ferroelectrics* **2008**, *368*, 63.
(14) Horiuchi, S.; Kumai, R.; Tokura, Y. *Chem. Commun.* **2007**, 2321.
(15) Czarnecki, P.; Nawrocik, W.; Pająk, Z.; Wąsicki, J. *Phys. Rev. B* **1994**, *49*, 1511.
(16) Czarnecki, P.; Nawrocik, W.; Pająk, Z.; Wąsicki, J. *J. Phys.: Condens. Matter* **1994**, *6*, 4955.
(17) Wąsicki, J.; Czarnecki, P.; Pająk, Z.; Nawrocik, W.; Szczepański, W. *J. Chem. Phys.* **1997**, *107*, 576.
(18) Pająk, Z.; Czarnecki, P.; Wąsicki, J.; Nawrocik, W. *J. Chem. Phys.* **1998**, *109*, 6420.
(19) Małuszyńska, H.; Czarnecki, P.; Lewicki, S.; Wąsicki, J.; Gdaniec, M. *J. Phys.: Condens. Matter* **2001**, *13*, 11053.
(20) Bobrowicz-Sarga, L.; Czarnecki, P.; Lewicki, S.; Natkaniec, I.; Nawrocik, W.; Wąsicki, J. *Phase Transitions* **2007**, *80*, 725.
(21) Wąsicki, J.; Pajzderska, A.; Fojud, Z. *J. Phys. Chem. C* **2008**, *112*, 7503–7508.
(22) Dutkiewicz, G.; Pająk, Z. *Z. Naturforsch.* **1998**, *53*, 1323.
(23) Miyoshi, T.; Kasano, H.; Mashiyama, H. *Ferroelectrics* **2007**, *346*, 130.
(24) Małuszyńska, H.; Scherf, Ch.; Czarnecki, P.; Cousson, A. *J. Phys.: Condens. Matter* **2003**, *15*, 5663.
(25) Prout, K.; Heyes, S. J.; Dobson, C. M.; McDaid, A.; Maris, T.; Muller, M.; Szaman, M. J. *Chem. Mater.* **2000**, *12*, 3561.
(26) Grottel, M.; Pajzderska, A.; Wąsicki, J. *Z. Naturforsch.* **2003**, *58a*, 638.
(27) Grottel, M.; Kozak, A.; Pajzderska, A.; Szczepański, W.; Wąsicki, J. *Z. Naturforsch.* **2004**, *59a*, 505.
(28) Małuszyńska, H.; Czarnecki, P. *Z. Kristallogr.* **2006**, *221*, 218.
(29) Pajzderska, A.; Fojud, Z.; Goc, R.; Wasicki, J. *J. Phys.: Condens. Matter* **2007**, *19*, 156220.
(30) Małuszynska, H.; Czarnecki, P.; Fojud, Z.; Wąsicki, J. *Acta Crystallogr., Sect. B* **2008**, *64*, 567.
(31) Pajzderska, A.; Gonzalez, M. A.; Wąsicki, J. *J. Chem. Phys.* **2008**, *128*, 084507.
(32) Bilski, P.; Bobrowicz-Sarga, L.; Czarnecki, P.; Małuszyńska, H.; Natkaniec, I.; Wąsicki, J. *J. Phys.: Condens. Matter* **2008**, *20*, 485222.
(33) Marczak, A.; Czarnecki, P.; Mielcarek, S. *Z. Naturforsch.* **2004**, *59a*, 857.
(34) Pajzderska, A.; Wąsicki, J.; Czarnecki, P.; Tupet, L.; Collet, E. *J. Chem. Phys.* **2009**, *130*, 044503.
(35) Aizu, K. *Phys. Rev. B* **1970**, *2*, 754–772.

(36) Hanaya, M.; Shibazaki, H.; Oguni, M.; Nemoto, T.; Ohashi, Y. *J. Phys. Chem. Solids* **2000**, *61*, 651–657.
(37) Pajzderska, A.; Gonzalez, M. A.; Wąsicki, J. Experimental report 7-03-66, 2008; club.ill.fr.
(38) Szafraniak, I.; Czarnecki, P.; Mayr, P. U.; Dollhopf, W. *Phys. Status Solidi* **1999**, *213*, 15–25.
(39) Pluta, T.; Sadlej, A. J. *J. Chem. Phys.* **2001**, *114*, 136.
(40) Masunov, A.; Dannenberg, J. J. *J. Phys. Chem. B* **2000**, *104*, 806.
(41) Czarnecki, P.; Katrusiak, A.; Szafraniak, I.; Wąsicki, J. *Phys. Rev. B* **1998**, *57*, 3326–3332.
(42) Czarnecki, P.; Małuszyńska, H. *J. Phys.: Condens. Matter* **2000**, *12*, 4881.
(43) Stankowska, J.; Czarnecka, A.; Mielcarek, S.; Słabolepsza, K. *Ferroelectrics* **1994**, *158*, 163–167.

JP9004295